Interaction of nanocarrier apoferritin with cytotoxic drug molecules

Simona Dostalova[1,2*], Monica Vazzana[1,3], Marketa Vaculovicova[1,2], Vojtech Adam[1,2] and Rene Kizek[4]

[1] Department of Chemistry and Biochemistry, Faculty of Agronomy, Mendel University in Brno, Zemedelska 1, CZ-613 00 Brno, Czech Republic, Emails: simona1dostalova@gmail.com (S.D.);; marketa.ryvolova@seznam.cz (M.V.); vojtech.adam@mendelu.cz (V.A.); kizek@sci.muni.cz (R.K.)

[2] Central European Institute of Technology, Brno University of Technology, Technicka 3058/10, CZ-616 00 Brno, Czech Republic

[3] Department of Biological and Environmental Sciences, University of Messina, Piazza Salvatore Pugliatti, 98122 Messina, Italy, Email: monicavazzana@libero.it (M.V.)

* Author to whom correspondence should be addressed; E-Mail: simona1dostalova@gmail.com; Tel.: +420-5-4513-3350; Fax: +420-5-4521-2044.

Received: 19.6.2015 / Accepted:19.6.2015 / Published: 1.10.2015

In this work, the encapsulation of cytotoxic drug doxorubicin (DOX) in protein nanocarrier apoferritin was studied. Two encapsulation protocols, using the disassembly and reassembly of apoferritin molecules in different surrounding pH and infusion method of encapsulation, were compared. The changes in size distribution and zeta potential of apoferritin in dependence to the pH changes, doxorubicin encapsulation and apoferritin:doxorubicin number of molecules ratio (1:14; 1:28; 1:56) were observed. The encapsulation efficiency at 1:56 apoferritin:doxorubicin ratio was 70% via pH changing method and 88% via infusion method. The release of doxorubicin molecules from nanocarrier after 14 days of storage at -20; 4; 20 and 37 °C was studied using capillary electrophoresis with laser induced fluorescence detection. The most stable was the storage at -20 °C with the infusion encapsulation method (after 14 days 0.32% DOX release). Due to very low release of cytotoxic drug molecules from apoferritin, apoferritin seems to be a suitable nanocarrier. Based on the size distribution changes, encapsulation efficiency and doxorubicin release, the infusion encapsulation method seems more promising.

Keywords: apoferritin; doxorubicin; fluorescence; nanocarrier; nanomedicine

1. Introduction

Naturally occurring or artificially prepared proteins can be employed in various fields including basic research [1-4], industry [5-8], immuno-based assays [9-12], detection of many different analytes [13-16], conventional medicine [17-20] or nanomedicine [21-24]. The first nanomedicine formulation ever approved by the FDA was a PEGylated bovine serum albumin in 1990, named Adagen® [25]. Out of the 44 FDA-approved nanomedicine formulations, 10 are polymer-protein conjugates or albumin nanoparticles [26-28] and novel protein-based nanocarriers are still being developed [29-32].

The use of proteins as nanocarriers has many advantages in comparison with artificial nanocarriers [33]. The immune response of patient's body to protein nanocarriers is much lower, especially for the proteins naturally occurring in humans or after surface modification with polyethyleneglycol [34]. Moreover, they can usually self-assemble to form uniform cages with an extraordinary binding capacity for various drugs. They are also biodegradable, and have abundant renewable sources [35]. The high binding capacity of protein nanocarriers owns to multiple functional groups in their primary sequence allowing for different interactions

with therapeutic molecules [36]. Drug molecules can also be reversibly encapsulated in some proteins' three-dimensional hollow cage [37].

The most frequently studied protein as a nanocarrier is a human serum albumin, the most abundant protein in blood plasma (about 60% of the total plasma protein count) [38]. Albumin is a globular protein containing 585 amino acids (with one tryptophan residue) and three homologous domains stabilized by disulfide bridges [39]. The ligands, either organic or inorganic, usually bind to the many hydrophobic cavities in albumin subdomains, making this protein an important regulator of intercellular fluxes and, moreover, drug behavior in vivo [40]. Ligands can interact with both C=O and C-N albumin groups, resulting in changes in its secondary structure [41]. Albumin nanoparticles were used for delivery of cytostatic drugs, siRNAs, vaccines or radiodiagnostics [42-45].

Protein apoferritin is also studied as a possible nanocarrier [29,46-48]. Apoferritin is also naturally found in human body as a major iron-binding protein. Apoferritin forms a hollow rhombic dodecahedral shell with outer diameter of 12-13 nm and an inner diameter of 7-8 nm [49]. The ligands can thus not only interact with amino acid residues of apoferritin but also be encapsulated in its hollow cavity. Many amino acid side chains of apoferritin 24 subunits interact to form hydrophobic cores, but there is also a large number of polar and hydrophilic residues, allowing for interaction with various molecules [50]. Some substances can bind to the apoferritin surface through hydrogen bonding (non-ionic molecules) or electrostatic interactions (ionic molecules) [51]. The apoferritin shell contains both hydrophobic and hydrophilic channels, allowing small molecules to enter the cavity via diffusion [52]. Its subunits can also be reversibly disassociated via the change of surrounding environment to encapsulate bigger molecules after reassembling [53]. In this work, we studied the interactions of cytotoxic drug doxorubicin with the apoferritin protein. Two encapsulation methods were compared, the pH changing and infusion method.

2. Results and Discussion

2.1 The encapsulation protocol

In this work, we studied the interactions of cytotoxic drug doxorubicin with protein nanocarrier apoferritin. To this end, two methods of doxorubicin encapsulation in apoferritin were evaluated. Fig. 1 shows the protocols of the two presented encapsulation methods. One of the methods employs the ability of apoferritin to reversibly disassociate its subunits in highly acidic pH and reassemble in the neutral pH, thus encapsulating any molecules mixed with disassembled apoferritin (Fig. 1A). The infusion method (Fig. 1B) allows the doxorubicin to enter the apoferritin cavity by diffusion through the channels in the apoferritin shell. The excess molecules of doxorubicin were removed in both methods by filtration through Amicon 3K centrifugal units.

2.2 The characterization of nanocarrier size and zeta potential

The influence of pH changes and doxorubicin encapsulation on the size distribution of created nanocarrier was evaluated (Fig. 2). In this experiment, the apoferritin:doxorubicin molecule ratio was 1:14. The native size of protein complex apoferritin in water (pH 6.9) was 16 nm with a small portion of 250 nm particles (Fig. 2A) and a zeta potential of -13.7 mV. Due to the pH changes, the structure of apoferritin was disassembled and reassembled, however, the reassembly process is not completely correct and part of the subunits can aggregated, creating nanoparticles of 160 nm or 5 000 nm in addition to the correctly reassembled 16 nm particles (Fig. 2B). The apoferritin was diluted in water after the disassembly/reassembly process and its zeta potential was -9.93 mV at pH 7.0.

After the encapsulation of doxorubicin via the pH changing method, particles of 16 nm and 300 nm were observed, with zeta potential of -19.5 mV at pH 7.2 (Fig. 2C). The size distribution of apoferritin with doxorubicin encapsulated via the infusion method was highly similar to the native apoferritin, with 16 nm particles and portion of 200 nm particles (Fig. 2D). However, the zeta potential of apoferritin with encapsu-

lated doxorubicin via the infusion method was decreased compared to native apoferritin, -19.5 mV at pH 7.3

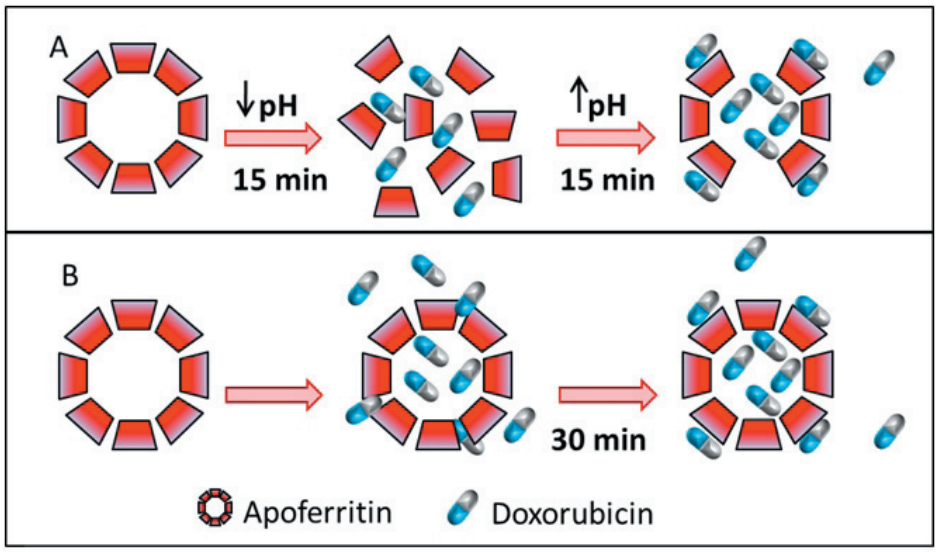

Figure 1: The encapsulation protocols compared in this work with subsequent removal of excess doxorubicin molecules by filtration through Amicon 3K centrifugal units at for 15 min at 25 °C and 6000×g and rinsing 3 times with water. (a) The encapsulation of doxorubicin molecules in apoferritin using the pH changing method. The apoferritin subunits were disassociated by acidification to pH 2.8 and mixed with doxorubicin for 15 min at 25 °C and 60 rpm. After that the pH was increased to 7.2 and the sample was mixed for 15 min at 25°C and 60 rpm to reassemble the apoferritin structure and allow the doxorubicin molecules to be encapsulated in apoferritin cavity. (b) The encapsulation of doxorubicin molecules in apoferritin using the infusion method. The apoferritin was mixed with doxorubicin for 30 min at 25 °C and 60 rpm.

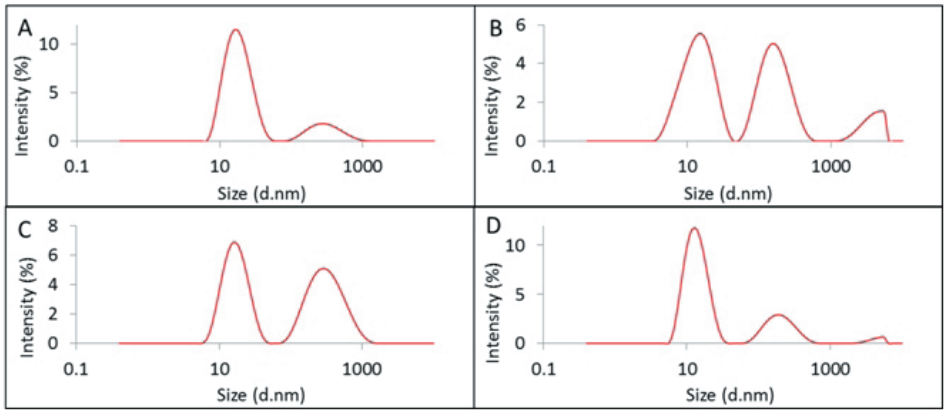

Figure 2: The changes of apoferritin size distribution by intensity due to the pH changes and doxorubicin encapsulation. (a) The size distribution by intensity of apoferritin in water, pH 6.9. (b) The size distribution by intensity of apoferritin in water after the pH changes, pH 7.0. (c) The size distribution by intensity of apoferritin with encapsulated doxorubicin via the pH changing method, pH 7.2. (d) The size distribution by intensity of apoferritin with encapsulated doxorubicin via the infusion method, pH 7.3.

The influence of apoferritin:doxorubicin ratio on the size distribution of created nanocarrier was further evaluated (Fig. 3). The size distribution of apoferritin with encapsulated doxorubicin via the pH changing encapsulation method changed with the increasing concentration of doxorubicin by increasing the portion of particles with 300 nm or more (Fig. 3A, C, E). However, no such changes in the size distribution were observed in the infusion encapsulation method with the increasing doxorubicin concentration (Fig. 3 B, D and F).

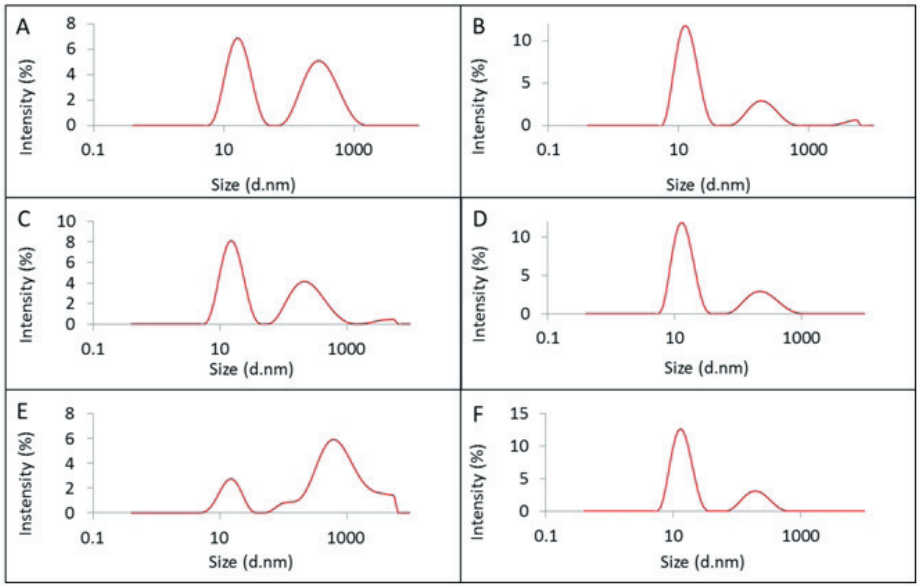

Figure 3: The changes of apoferritin size distribution by intensity due to the different apoferritin:doxorubicin ratio during encapsulation. (**a, c, e**) The size distribution by intensity of apoferritin with encapsulated doxorubicin via the pH changing method (**b, d, f**) The size distribution by intensity of apoferritin with encapsulated doxorubicin via the infusion method. (**a, b**) The apoferritin:doxorubicin ratio 1:14. (**c, d**) The apoferritin:doxorubicin ratio 1:28. (**e, f**) The apoferritin:doxorubicin ratio 1:56.

2.3 The efficiency of doxorubicin encapsulation in apoferritin nanocarrier using different methods

To evaluate the encapsulation efficiency the optical properties of doxorubicin were used – its absorption maximum at 480 nm and emission maximum at 600 nm. Absorbance and fluorescence spectra of created nanocarriers were measured after the encapsulation of doxorubicin molecules in apoferritin via the pH changing and infusion method and subsequent removal of excess doxorubicin molecules (Fig. 4). The apoferritin:doxorubicin molecule ratio was 1:56.

Following encapsulation, both the absorbance and fluorescence of doxorubicin is significantly decreased. Fig. 4A shows the decrease of doxorubicin absorbance after the encapsulation very similarly in both encapsulation methods, 1.95× using the infusion encapsulation method and 2× using the pH changing method. The decrease of doxorubicin fluorescence was also observed (Fig. 4B) and it differed significantly between the individual encapsulation methods – 6.61× decrease of fluorescence using the infusion method and 7.4× using the pH changing method.

After the subsequent removal of excess doxorubicin molecules by filtration and adjusting the sample volume to original, the absorbance (Fig. 4C) and fluorescence (Fig. 4D) spectra were measured again. After comparison with absorbance and fluorescence spectra before filtration, it was observed that 88% of doxorubi-

cin molecules were encapsulated in apoferritin using the infusion method, while only 70% were encapsulated using the pH changing method.

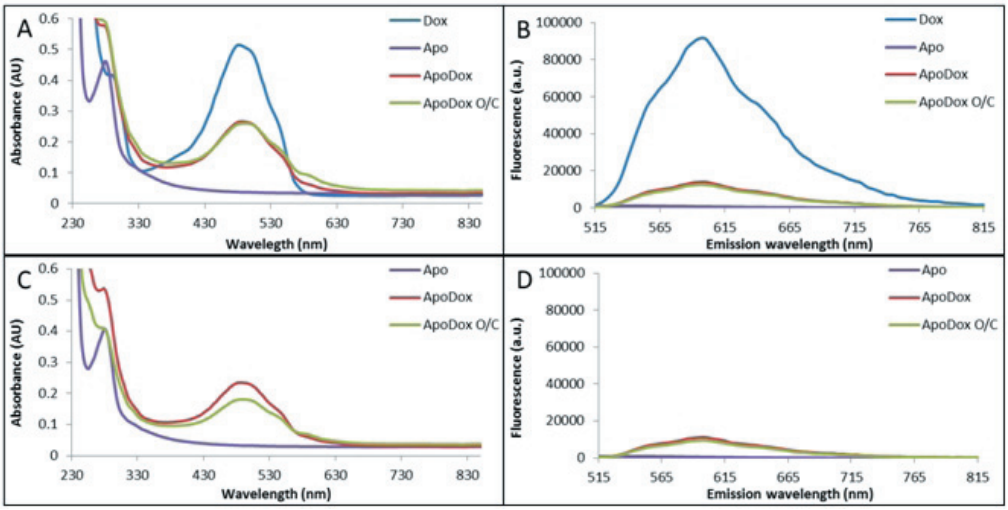

Figure 4: The absorbance (**a, c**) and emission (**b, d**) spectra of apoferritin with encapsulated doxorubicin via the pH changing (ApoDox O/C) and infusion (ApoDox) method after encapsulation (**a, b**) and after subsequent removal of excess doxorubicin molecules (**c, d**). The apoferritin:doxorubicin ratio was 1:56. Emission was measured at excitation wavelength 480 nm.

2.4 The release of doxorubicin molecules from apoferritin during a long-term storage

To evaluate the apoferritin stability the release of doxorubicin molecules from apoferritin during a storage for 14 days at different temperatures (-20; 4; 20 and 37 °C) was observed using capillary electrophoresis with laser induced fluorescence detection. In contrast to known literature [29,48] it was observed that, following encapsulation, part of doxorubicin molecules is located inside the apoferritin cavity and part on its surface. This is concluded based on the change in zeta potential of apoferritin after encapsulation of doxorubicin and by the behavior of apoferritin with encapsulated doxorubicin in electric field (Fig. 5). Doxorubicin showed two distinct peaks after separation in capillary electrophoresis (Fig. 5A). Apoferritin with encapsulated doxorubicin via both encapsulation methods showed a third peak with electrophoretic mobility corresponding to apoferritin in addition to the two peaks corresponding to doxorubicin (Fig. 5B). During the separation by capillary electrophoresis the doxorubicin molecules from the apoferritin surface are probably released by the surrounding electric field [54]. This behavior was observed in apoferritin with encapsulated doxorubicin via both pH changing and infusion method.

The height of peak corresponding to apoferritin with encapsulated doxorubicin after 1; 2; 3; 6; 10 and 14 days of storage was used to compare the release from nanocarriers prepared via different encapsulation methods and storage at different temperatures (Fig. 6). After 6 days of storage in all temperatures, the peak height of apoferritin with encapsulated doxorubicin was increased which can be caused by the transfer of more doxorubicin molecules from the apoferritin surface to its cavity. After longer storage the release of doxorubicin molecules from apoferritin cavity is very limited. The encapsulation of doxorubicin via the pH changing method caused higher (2.7×) release of doxorubicin molecules from apoferritin (Fig. 6A-D). This can probably be caused by the fact, that reassembly of apoferritin after pH changes is not complete but there appear two hole defects on opposite apoferritin poles [53] and

doxorubicin can leave the apoferritin cavity through these defects.

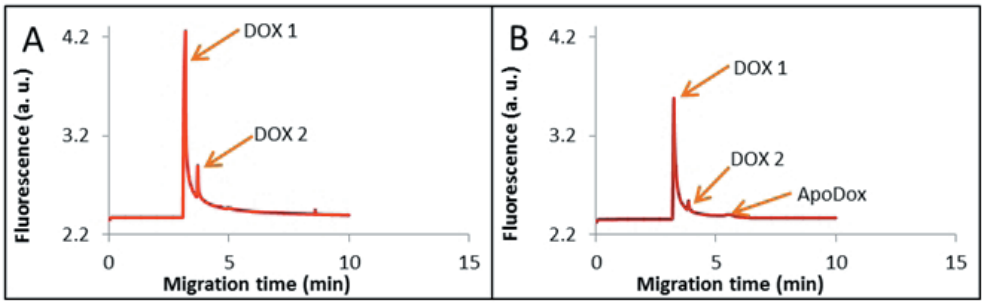

Figure 5: The behavior of doxorubicin (**a**) and apoferritin with encapsulated doxorubicin via both the pH changing and infusion method (**b**) during capillary electrophoresis with laser induced fluorescence detection using fused silica capillary with internal diameter of 75 μm and total length of 64.5 cm (54 cm to detector window); the separation voltage of 20 kV and hydrodynamic injection by 3 psi for 10 s.

The lowest release was observed after storage at -20 °C with 0.75% of released doxorubicin encapsulated via the pH changing method (Fig. 6A) and 0.32% via the infusion method (Fig. 6E) after 14 days of storage. Thus it can be concluded, that apoferritin with encapsulated doxorubicin is the most stable after storage at -20 °C. After 14 days of storage at 4 °C, the release was 1.67% with encapsulation via pH changing method (Fig. 6B) and 0.29% via the infusion method (Fig. 6F). The highest release and thus the lowest stability was observed after storage at 20 °C, with 2.44% of released molecules with encapsulation via pH changing method (Fig. 6C) and 2.02% via infusion method (Fig. 6G). After 14 days of storage at 37 °C, 1.47% of doxorubicin was released with encapsulation via pH changing method (Fig. 6D) and 1% via the infusion method (Fig. 6H).

3. Experimental Section

3.1 Chemicals

All chemicals of ACS purity were obtained from Sigma-Aldrich (St. Louis, MO, USA) unless stated otherwise. The deionized water was prepared using reverse osmosis equipment Aqual 25 (Aqual s.r.o., Brno, Czech Republic). The deionized water was further purified by using apparatus Milli-Q Direct QUV equipped with an UV lamp from Millipore (Billerica, MA, USA), exhibiting a resistance of 18 MΩ. The pH was measured using pH meter WTW inoLab (Weilheim, Germany).

3.2 The encapsulation of doxorubicin in apoferritin via pH changing method

1 mg of apoferritin (20 μL of 50 mg/mL) was mixed with 67.2 μg of doxorubicin (200 μL of 336 μg/mL) with a molar ratio of apoferritin:-doxororubicin 1:56 and 100 μL of water. Using 2.5 μL of 1 M HCl the pH was lowered to 2.8 to disassociate the apoferritin subunits. The sample was mixed for 15 min at 25 °C and 60 rpm. The pH was changed to 7.2 with 2.7 μL of 1M NaOH and the sample was shaken for 15 min at 25 °C and 60 rpm to reassemble the subunits and encapsulate the doxorubicin in apoferritin hollow. The excess doxorubicin molecules were removed by filtration using the centrifugation in Amicon 3K centrifugal units for 15 min at 25 °C and 6000×g. The samples were rinsed with water 3 times. Water was added after the filtration to fill the sample to its original volume.

3.3 The encapsulation of doxorubicin in apoferritin via infusion method

1 mg of apoferritin (20 μL of 50 mg/mL) was mixed with 67.2 μg of doxorubicin (200 μL of 336 μg/mL) with a molar ratio of apoferritin:-doxororubicin 1:56 and 100 μL of water.

The sample was shaken for 30 min at 25 °C and 60 rpm. The excess doxorubicin molecules were removed by filtration using the centrifugation in Amicon 3K centrifugal units for 15 min at 25 °C and 6000×g. The samples were rinsed

with water 3 times. Water was added after the filtration to fill the sample to its original volume.

in apoferritin was evaluated using the optical properties of doxorubicin. The absorbance (wavelength 230-850 nm) and fluorescence

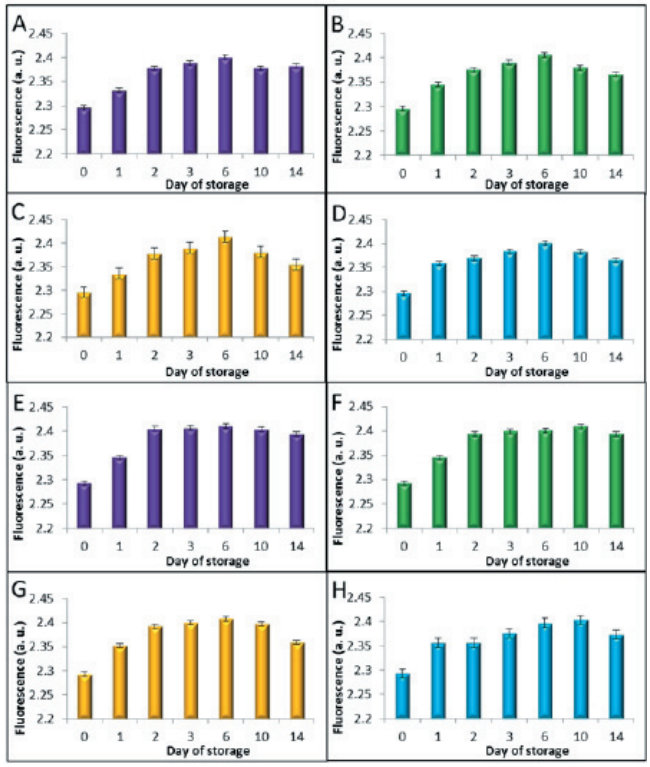

Figure 6: The release of doxorubicin from apoferritin nanocarrier during 14 days of storage at -20 °C (**a, e**), 4 °C (**b, f**); 20 °C (**c, g**) and 37 °C (**d, h**). The encapsulation was performed via both the pH changing (a-d) and infusion method (**e-h**). The release was measured using fused silica capillary with internal diameter of 75 μm and total length of 64.5 cm (54 cm to detector window); the separation voltage of 20 kV and hydrodynamic injection by 3 psi for 10 s.

3.4 Characterization of nanocarrier size

The average particle size and size distribution were determined by quasi elastic laser light scattering with a Malvern Zetasizer (NANO-ZS, Malvern Instruments Ltd., Worcestershire, United Kingdom). The zeta potential was determined by laser Doppler micro-electrophoresis with a Malvern Zetasizer. Nanoparticles in distilled water solution of 1.5 mL were put into a polystyrene latex cell and measured at a detector angle of 173°, a wavelength of 633 nm, temperature 25 °C and a refractive index of 1.33.

3.5 The encapsulation efficiency

The efficiency of doxorubicin encapsulation

(excitation wavelength 480 nm, emission 515-815 nm) spectra of the resulting nanocarriers were measured using the TECAN Infinite 200 PRO microtitration plate reader (Männedorf, Switzerland).

3.6 The release of doxorubicin molecules from apoferritin nanocarrier during 14 days

The created apoferritin nanocarrier with encapsulated doxorubicin using both pH changing and infusion encapsulation method was stored for 14 days at -20; 4; 20 and 37 °C. After 1; 2; 3; 6; 10 and 14 days of storage the nanocarrier fluorescence was measured using the capillary electrophoresis with laser induced fluorescence

detection CE 7100, Agilent Technologies (Santa Clara, CA, USA). Fused silica capillary with internal diameter of 75 µm and with the total length of 64.5 cm (54 cm to detector window) was used. The separation voltage of 20 kV and hydrodynamic injection by 3 psi for 10 s was employed.

4. Conclusions

Two methods for doxorubicin encapsulation in apoferritin nanocarrier were compared in this study. Standard, pH changing method showed 70% encapsulation efficiency, while the infusion method showed 88% encapsulation efficiency. A very low release of doxorubicin molecules from apoferritin nanocarrier after storage for 14 days at different temperatures was observed with the most stable using the infusion encapsulation method and storage at -20 °C.

Acknowledgments

The authors gratefully acknowledge financial support from the Grant Agency of the Czech Republic (NANOCHEMO GA CR 14-18344S) and PGS28_2014.

Conflicts of Interest

The authors declare they have no potential conflicts of interests concerning drugs, products,services or another research outputs in this study. The Editorial Board declares that the manuscript met the ICMJE „uniform reguirements“ for biomedical papers.

References

1. Chayaratanasin, P.; Barbieri, M.A.; Suanpairintr, N.; Adisakwattana, S. Inhibitory effect of clitoria ternatea flower petal extract on fructose-induced protein glycation and oxidation-dependent damages to albumin in vitro. BMC complementary and alternative medicine 2015, 15, 546.
2. Kim, K.-W.; Kim, B.-M.; Moon, H.-W.; Lee, S.-H.; Kim, H.-R. Role of c-reactive protein in osteoclastogenesis in rheumatoid arthritis. Arthritis research & therapy 2015, 17, 563.
3. Moran, G.; Carcamo, C.; Concha, M.; Folch, H. Expression of the protein serum amyloid a in response to aspergillus fumigatus in murine models of allergic airway inflammation. Rev. Iberoam. Micol. 2015, 32, 25-29.
4. Tsushima, H.; Okazaki, K.; Ishihara, K.; Ushijima, T.; Iwamoto, Y. Ccaat/enhancer-binding protein beta promotes receptor activator of nuclear factor-kappa-b ligand (rankl) expression and osteoclast formation in the synovium in rheumatoid arthritis. Arthritis research & therapy 2015, 17, 532.
5. Fujiwara, M.; Imura, T. Transparent silica thin films prepared from sodium silicate and bovine serum albumin with petal effect. Ceram. Int. 2015, 41, 7565-7572.
6. Rasala, B.A.; Mayfield, S.P. Photosynthetic biomanufacturing in green algae; production of recombinant proteins for industrial, nutritional, and medical uses. Photosynth. Res. 2015, 123, 227-239.
7. Zhao, Y.; Zhao, Y.Z.; Xu, H.L.; Yang, Y.Q. A sustainable slashing industry using biodegradable sizes from modified soy protein to replace petro-based poly(vinyl alcohol). Environ. Sci. Technol. 2015, 49, 2391-2397.
8. Zhao, Y.Z.; Zhao, Y.; Yang, Y.Q. Modified soy protein to substitute non-degradable petrochemicals for slashing industry. Ind. Crop. Prod. 2015, 67, 466-474.
9. Heger, Z.; Cernei, N.; Krizkova, S.; Masarik, M.; Kopel, P.; Hodek, P.; Zitka, O.; Adam, V.; Kizek, R. Paramagnetic nanoparticles as a platform for fret-based sarcosine picomolar detection. Sci Rep 2015, 5.
10. Krizkova, S.; Ryvolova, M.; Hynek, D.; Eckschlager, T.; Hodek, P.; Masarik, M.; Adam, V.; Kizek, R. Immunoextraction of zinc proteins from human plasma using chicken yolk antibodies immobilized onto paramagnetic particles and their electrophoretic analysis. Electrophoresis 2012, 33, 1824-1832.
11. Van Zoelen, S.A.; Ozkan, O.; Inceoglu, B. Antigenic cross-reactivity anti-birtoxin antibody against androctonus crassicauda venom. J. Arthropod.-Borne Dis. 2015, 9, 176-183.
12. Zitka, O.; Krizkova, S.; Skalickova, S.; Dospivova, D.; Adam, V.; Kizek, R. Microfluidic tool coupled with electrochemical assay for detection of lactoferrin isolated by antibody-modified paramagnetic beads. Electrophoresis 2013, 34, 2120-2128.
13. Abdelwahab, M.; Loa, C.C.; Wu, C.C.; Lin, T.L. Recombinant nucleocapsid protein-based enzyme-linked immunosorbent assay for detection of antibody to turkey coronavirus. J. Virol. Methods 2015, 217, 36-41.
14. Heger, Z.; Zitka, O.; Fohlerova, Z.; Rodrigo, M.A.M.; Hubalek, J.; Kizek, R.; Adam, V. Use of green fluorescent proteins for in vitro biosensing. Chem. Pap. 2015, 69, 54-61.
15. Minnaard, M.C.; Van De Pol, A.C.; De Groot, J.A.H.; De Wit, N.J.; Hopstaken, R.M.; Van Delft, S.; Goossens, H.; Ieven, M.; Lammens, C.; Little, P., et al. The added diagnostic value of five different c-reactive protein point-of-care test devices in detecting pneumonia in primary care: A nested case-control study. Scand. J. Clin. Lab. Invest. 2015, 75, 291-295.
16. Sonaimuthu, P.; Cheong, F.W.; Chin, L.C.; Mahmud, R.; Fong, M.Y.; Lau, Y.L. Detection of human malaria using recombinant plasmodium knowlesi merozoire surface protein-1 (msp-119) expressed in escherichia coli. Experimental parasitology 2015, 153, 118-122.
17. Kassir, R.; Blanc, P.; Tibalbo, L.M.B.; Breton, C.;

Lointier, P. C-reactive protein and procalcitonin for the early detection of postoperative complications after sleeve gastrectomy: Preliminary study in 97 patients. Surg. Endosc. 2015, 29, 1439-1444.
18. Liyasova, M.S.; Ma, K.; Lipkowitz, S. Molecular pathways: Cbl proteins in tumorigenesis and antitumor immunity-opportunities for cancer treatment. Clin. Cancer Res. 2015, 21, 1789-1794.
19. Numbenjapon, N.; Chamnanwanakij, S.; Sangaroon, P.; Simasathien, S.; Watanaveeradej, V. C-reactive protein as a single useful parameter for discontinuation of antibiotic treatment in thai neonates with clinical sepsis. Journal of the Medical Association of Thailand = Chotmaihet thangphaet 2015, 98, 352-357.
20. Zali, H.; Zamanian-Azodi, M.; Tavirani, M.R.; Baghban, A.A.Z. Protein drug targets of lavandula angustifolia on treatment of rat alzheimer's disease. Iran. J. Pharm. Res. 2015, 14, 291-302.
21. Heger, Z.; Cernei, N.; Blazkova, I.; Kopel, P.; Masarik, M.; Zitka, O.; Adam, V.; Kizek, R. Gammafe2o3 nanoparticles covered with glutathione-modified quantum dots as a fluorescent nanotransporter. Chromatographia 2014, 77, 1415-1423.
22. Janu, L.; Stanisavljevic, M.; Krizkova, S.; Sobrova, P.; Vaculovicova, M.; Kizek, R.; Adam, V. Electrophoretic study of peptide-mediated quantum dot-human immunoglobulin bioconjugation. Electrophoresis 2013, 34, 2725-2732.
23. Rodrigues, S.; Cordeiro, C.; Seijo, B.; Remunan-Lopez, C.; Grenha, A. Hybrid nanosystems based on natural polymers as protein carriers for respiratory delivery: Stability and toxicological evaluation. Carbohydr. Polym. 2015, 123, 369-380.
24. Sahebalzamani, M.; Biazar, E.; Shahrezaei, M.; Hosseinkazemi, H.; Rahiminavaie, H. Surface modification of phbv nanofibrous mat by laminin protein and its cellular study. Int. J. Polym. Mater. Polym. Biomat. 2015, 64, 149-154.
25. Syiam, M.M.; El-Aziem, M.A.; Soliman, M.E.M. Adagen: Adaptive interface agent for x-ray fracture detection. Ieee: New York, 2004; p 354-357.
26. Alconcel, S.N.S.; Baas, A.S.; Maynard, H.D. Fda-approved poly(ethylene glycol)-protein conjugate drugs. Polym. Chem. 2011, 2, 1442-1448.
27. Gommans, G.M.M.; Boer, R.O.; van Dongen, B.A.; van der Schors, T.G.; de Waard, J.W.D. Optimisation of 99mtc-nanocoll sentinel node localisation in carcinoma of the breast. Eur. J. Nucl. Med. 2000, 27, 744-744.
28. O'Shaughnessy, J.A.; Blum, J.L.; Sandbach, J.F.; Savin, M.; Fenske, E.; Hawkins, M.J.; Baylor-Charles, A. Weekly nanoparticle albumin paclitaxel (abraxane) results in long-term disease control in patients with taxane-refractory metastatic breast cancer. Breast Cancer Res. Treat. 2004, 88, S65-S65.
29. Blazkova, I.; Nguyen, V.H.; Dostalova, S.; Kopel, P.; Stanisavljevic, M.; Vaculovicova, M.; Stiborova, M.; Eckschlager, T.; Kizek, R.; Adam, V. Apoferritin modified magnetic particles as doxorubicin carriers for anticancer drug delivery. Int. J. Mol. Sci. 2013, 14, 13391-13402.
30. Chen, C.H.; Hu, H.Y.; Qiao, M.X.; Zhao, X.L.; Wang, Y.J.; Chen, K.; Chen, D.W. Anti-tumor activity of paclitaxel through dual-targeting lipoprotein-mimicking nanocarrier. J. Drug Target. 2015, 23, 311-322.
31. Mottaghitalab, F.; Farokhi, M.; Shokrgozar, M.A.; Atyabi, F.; Hosseinkhani, H. Silk fibroin nanoparticle as a novel drug delivery system. J. Control. Release 2015, 206, 161-176.
32. Zhou, Z.L.; Badkas, A.; Stevenson, M.; Lee, J.Y.; Leung, Y.K. Herceptin conjugated plga-phis-peg ph sensitive nanoparticles for targeted and controlled drug delivery. Int. J. Pharm. 2015, 487, 81-90.
33. Dostalova, S.; Munzova, D.; Vaculovicova, M.; Kizek, R. Delivery of doxorubicin using protein nanocarriers. J. Metallomics Nanotech. 2014, 1, 34-38.
34. Ma, Y.J.; Nolte, R.J.M.; Cornelissen, J. Virus-based nanocarriers for drug delivery. Adv. Drug Deliv. Rev. 2012, 64, 811-825.
35. Elzoghby, A.O.; Samy, W.M.; Elgindy, N.A. Protein-based nanocarriers as promising drug and gene delivery systems. J. Control. Release 2012, 161, 38-49.
36. Elzoghby, A.O.; Samy, W.M.; Elgindy, N.A. Albumin-based nanoparticles as potential controlled release drug delivery systems. J. Control. Release 2012, 157, 168-182.
37. Elzoghby, A.O.; El-Fotoh, W.S.A.; Elgindy, N.A. Casein-based formulations as promising controlled release drug delivery systems. J. Control. Release 2011, 153, 206-216.
38. Chen, T.; Zhu, X.; Chen, Q.; Ge, M.; Jia, X.; Wang, X.; Ge, C. Interaction between z-ligustilide from radix angelica sinensis and human serum albumin. Food Chem. 2015, 186, 292-297.
39. Sugio, S.; Kashima, A.; Mochizuki, S.; Noda, M.; Kobayashi, K. Crystal structure of human serum albumin at 2.5 angstrom resolution. Protein Eng. 1999, 12, 439-446.
40. Varshney, A.; Rehan, M.; Subbarao, N.; Rabbani, G.; Khan, R.H. Elimination of endogenous toxin, creatinine from blood plasma depends on albumin conformation: Site specific uremic toxicity & impaired drug binding. PLoS One 2011, 6.
41. Liu, Y.; Chen, M.M.; Jiang, L.G.; Song, L. Stereoselective interaction of cinchona alkaloid isomers with bovine serum albumin. Food Chem. 2015, 181, 170-178.
42. Kunda, N.K.; Alfagih, I.M.; Dennison, S.R.; Tawfeek, H.M.; Somavarapu, S.; Hutcheon, G.A.; Saleem, I.Y. Bovine serum albumin adsorbed pga-co-pdl nanocarriers for vaccine delivery via dry powder inhalation. Pharm. Res. 2015, 32, 1341-1353.
43. Sharma, R.I.; Pereira, M.; Schwarzbauer, J.E.; Moghe, P.V. Albumin-derived nanocarriers: Substrates for enhanced cell adhesive ligand display and cell motility. Biomaterials 2006, 27, 3589-3598.
44. Son, S.; Song, S.; Lee, S.J.; Min, S.; Kim, S.A.; Yhee, J.Y.; Huh, M.S.; Kwon, I.C.; Jeong, S.Y.; Byun, Y., et al. Self-crosslinked human serum albumin nanocarriers for systemic delivery of polymerized sirna to tumors. Biomaterials 2013, 34, 9475-9485.
45. Yuan, A.; Wu, J.H.; Song, C.C.; Tang, X.L.; Qiao,

Q.; Zhao, L.L.; Gong, G.M.; Hu, Y.Q. A novel self-assembly albumin nanocarrier for reducing doxorubicin-mediated cardiotoxicity. J. Pharm. Sci. 2013, 102, 1626-1635.
46. Heger, Z.; Skalickova, S.; Zitka, O.; Adam, V.; Kizek, R. Apoferritin applications in nanomedicine. Nanomedicine 2014, 9, 2233-2245.
47. Munzova, D.; Dostalova, S.; Vaculovicova, M.; Kizek, R. Apoferritin: Nanocarrier for targeted drug delivery. J. Metallomics Nanotech. 2014, 1, 50-54.
48. Tmejova, K.; Hynek, D.; Kopel, P.; Dostalova, S.; Smerkova, K.; Stanisavljevic, M.; Nguyen, V.H.; Nejdl, L.; Vaculovicova, M.; Krizkova, S., et al. Electrochemical behaviour of doxorubicin encapsulated in apoferritin. Int. J. Electrochem. Sci. 2013, 8, 12658-12671.
49. Haussler, W. Structure and dynamics in apoferritin solutions with paracrystalline order. Chem. Phys. 2003, 292, 425-434.
50. Crichton, R.R.; Declercq, J.P. X-ray structures of ferritins and related proteins. Biochim. Biophys. Acta-Gen. Subj. 2010, 1800, 706-718.
51. Liu, F.; Du, B.J.; Chai, Z.; Zhao, G.H.; Ren, F.Z.; Leng, X.J. Binding properties of apoferritin to nicotinamide and calcium. Eur. Food Res. Technol. 2012, 235, 893-899.
52. Granier, T.; Gallois, B.; Dautant, A.; Destaintot, B.L.; Precigoux, G. Comparison of the structures of the cubic and tetragonal forms of horse-spleen apoferritin. Acta Crystallogr. Sect. D-Biol. Crystallogr. 1997, 53, 580-587.
53. Kim, M.; Rho, Y.; Jin, K.S.; Ahn, B.; Jung, S.; Kim, H.; Ree, M. Ph-dependent structures of ferritin and apoferritin in solution: Disassembly and reassembly. Biomacromolecules 2011, 12, 1629-1640.
54. Konecna, R.; Nguyen, H.V.; Stanisavljevic, M.; Blazkova, I.; Krizkova, S.; Vaculovicova, M.; Stiborova, M.; Eckschlager, T.; Zitka, O.; Adam, V., et al. Doxorubicin encapsulation investigated by capillary electrophoresis with laser-induced fluorescence detection. Chromatographia 2014, 77, 1469-1476.